Electronic Supplementary Material (ESI)

Rapid Reversible Borane to Boryl Hydride Exchange by Metal Shuttling on the Carborane Cluster Surface

Bennett J. Eleazer[a], Mark D. Smith[a], Alexey A. Popov[b]*, and Dmitry V. Peryshkov[a]*.

a). Department of Chemistry and Biochemistry, University of South Carolina, 631 Sumter St., Columbia, South Carolina 29208, United States.
b). Leibniz Institute for Solid State and Materials Research, Helmholtzstrasse 20, 01069 Dresden, Germany.

Experimental

All synthetic manipulations were carried out either in a nitrogen-filled drybox or on an air-free dual-manifold Schlenk line, unless stated otherwise. Compounds **2** and **3** were found to be moderately stable on air in a solid state. The solvents were sparged with nitrogen, passed through activated alumina, and stored over activated 4 Å Linde-type molecular sieves. Benzene-*d*$_6$ was degassed and stored over activated 4 Å Linde-type molecular sieves. NMR spectra were recorded using Varian spectrometers at 400 (^{1}H), 100 (^{13}C), 162 (^{31}P), 128 (^{11}B) MHz, reported in δ (parts per million) and referenced to the residual ^{1}H/^{13}C signals of the deuterated solvent or an external 85% H_3PO_4 (^{31}P (δ): 0.0 ppm) and $BF_3(Et_2O)$ (^{11}B(δ): 0.0 ppm) standards. J values are given in Hz. Midwest Microlab, Indianapolis, Indiana provided the elemental analysis results.

POBOP-H ligand precursor (POBOP = 1,7-OP(*i*-Pr)$_2$-*m*-2-carboranyl) was prepared using the previously reported procedure.[1] $Ru(PPh_3)_3Cl_2$ (Strem), *m*-carborane $C_2B_{10}H_{12}$ (Katchem), cyclooctane, t-butylethylene, and *n*-octane-*d*$_{18}$ (Alfa Aesar) were used as received. Sodium hydride oil suspension was washed with hexanes to produce white powder.

Synthesis of (POBOP)Ru(Cl)(PPh$_3$) complex (2)

A portion of $RuCl_2(PPh_3)_3$ (0.116 g; 0.121 mmol) was added to a solution of (POBOP)H (0.050 g; 0.122 mmol) in THF (10 mL). The dark brown reaction mixture was transferred to a storage tube and heated under reflux for 16 hours (oil bath temperature 90 ºC). The resulting solution was dried under vacuum, triturated with acetonitrile, and filtered. The filtrate was evaporated and recrystallized from a mixture of diethyl ether and hexanes at –30 °C to produce an orange crystalline product. Yield: 0.085 g, 0.105 mmol, 86%.

^{1}H (C_6D_6): δ 8.38 (br, 6H, $P(C_6H_6)_3$), 6.95 (br, 9H, $P(C_6H_6)_3$), 4.0–1.5 (br m, 10H, B*H*), 2.20 (m, 2H, $P(CH(CH_3)_2)$), 1.73 (m, 6H, $P(CH(CH_3)_2)$), 1.20 (m, 6H, $P(CH(CH_3)_2)$), 0.66 (m, 6H, $P(CH(CH_3)_2)$), 0.56 (overlapping m, 6H, $P(CH(CH_3)_2$ and m, 2H, $P(CH(CH_3)_2)$), –5.44 (q, 1H, $^1J_{BH}$ = 116 Hz, B–*H*···Ru). **^{11}B{^{1}H}** (C_6D_6): δ –1.8 (Ru–*B*), –12.9, –15.1, –19.9, –21.3. **^{13}C (C_6D_6):** δ 134.4 ($P(C_6H_5)_3$, 127.0 134.4 ($P(C_6H_5)_3$, 111.1 ($C_2B_{10}H_8$), 34.1 ($P(CH(CH_3)_2)$, 27.7 ($P(CH(CH_3)_2)$, 19.3 ($P(CH(CH_3)_2)$, 17.5 ($P(CH(CH_3)_2)$, 15.9 ($P(CH(CH_3)_2)$, 15.5 ($P(CH(CH_3)_2)$. **^{31}P{^{1}H} (C_6D_6):** δ 196.8 (d, 2P, $^2J_{PP}$ = 40 Hz, $P(CH(CH_3)_2)$, 56.3 (br, 1P, $P(C_6H_6)_3$). Found: C, 47.72; H, 6.55. Calcd. for $C_{32}H_{52}B_{10}ClO_2P_3Ru$: C, 47.67; H, 6.50.

Synthesis of (POBOP)Ru(H)(PPh$_3$) complex (3)

A portion of NaH (0.002 g; 0.083 mmol) was added to a solution of (POBOP)Ru(Cl)(PPh$_3$) (0.060 g; 0.074 mmol) in THF (2 mL). The resulting suspension was transferred to a J. Young valve NMR tube and heated at 75 °C for 36 hours. The dark brown solution was then filtered and dried under vacuum. The product was recrystallized from diethyl ether. Yield: 0.056 g, 0.073 mmol, 98%

^{1}H NMR (CD_2Cl_2): δ 7.72 (m, 6H, $P(C_6\mathit{H}_5)_3$), 7.35 (m, 9H, $P(C_6\mathit{H}_5)_3$), 3.5 to 0.5 (br, 9H, $C_2B_{10}\mathit{H}_9$), 1.38 (m, 4H, $P(C\mathit{H}(CH_3)_2)$, 0.87 (m, 12H, $P(C\mathit{H}(CH_3)_2)$, 0.80 (m, 12H, $P(CH(C\mathit{H}_3)_2))$, –8.95 (br, 2H, Ru–*H*/B–*H*···Ru). **^{11}B{^{1}H} (CD_2Cl_2):** δ –8.2 (*B*–Ru/*B*–H···Ru), –13.5 (*B*H), –17.3 (*B*H). **^{13}C (CD_2Cl_2):** δ 134.5 (d, $^3J_{PC}$ = 12 Hz, $P(\mathit{C}_6H_5)_3$), 129.2 ($P(\mathit{C}_6H_5)_3$), 127.5 (d, $^2J_{PC}$ = 8 Hz, $P(\mathit{C}_6H_5)_3$), 30.2 ($P(\mathit{C}H(CH_3)_2)$, 19.0 ($P(CH(\mathit{C}H_3)_2)$, 17.2 ($P(CH(\mathit{C}H_3)_2)$. **^{31}P{^{1}H} (CD_2Cl_2):** δ 221.7 (d, $^2J_{PP}$ = 17 Hz, 2P, $P(CH(C\mathit{H}_3)_2)$, 52.0 (br, 1P, $P(C_6H_5)_3$). Found: C, 49.51; H, 6.86. Calcd. for $C_{32}H_{53}B_{10}O_2P_3Ru$: C, 49.79; H, 6.92.

Catalytic dehydrogenation studies

COA:TBE:catalyst molar ratio of 5700:1000:1

A portion of $(POBOP)Ru(H)(PPh_3)$ (0.008 g, 0.010 mmol) and naphthalene (0.128 g, 1.0 mmol) was dissolved in 1 mL of C_6D_6. Neat cyclooctane (4.71 mL, 0.057 mol) and tertbutylethylene (1.29 mL, 0.010 mol) were then added to the catalyst solution. Aliquots (0.30 mL) of the resulting stock solution were transferred to NMR tubes and flame-sealed under nitrogen or air. The tubes were heated at 170 ºC in an oil bath for a set time period (1h or 2h). TONs were calculated on the basis of integral intensities of signals of cyclooctene and naphthalene (internal standard) in the ^{1}H NMR spectra.

COA:TBE:catalyst molar ratio of 3000:3000:1

A portion of $(POBOP)Ru(H)(PPh_3)$ (0.005 g, 0.006 mmol) and naphthalene (0.066 g, 0.51 mmol) was dissolved in 1 mL of C_6D_6. Neat cyclooctane (2.61 mL, 0.019 mol) and tert-butylethylene (2.5 mL, 0.019 mol) were then added to the catalyst solution. Aliquots (0.30 mL) of the resulting stock solution were transferred to NMR tubes and flame-sealed under nitrogen or air. The tubes were heated at 170 ºC in an oil bath for a set time period (1h or 2h). TONs were calculated on the basis of integral intensities of signals of cyclooctene and naphthalene (internal standard) in the ^{1}H NMR spectra.

References:

1. Eleazer, B. J.; Smith, M. D.; Peryshkov, D. V. *Organometallics*, **2016**, *35*, 106–112.

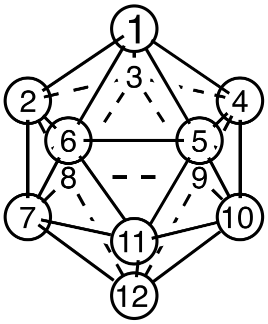

Figure S-1. The numbering scheme for the icosahedral *closo*-carborane cluster. For the *m*-$C_2B_{10}H_{12}$, carbon atoms are at positions 1 and 7.

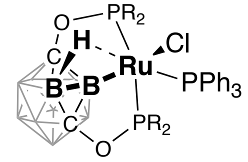

(POBOP)Ru(Cl)(PPh$_3$)

2

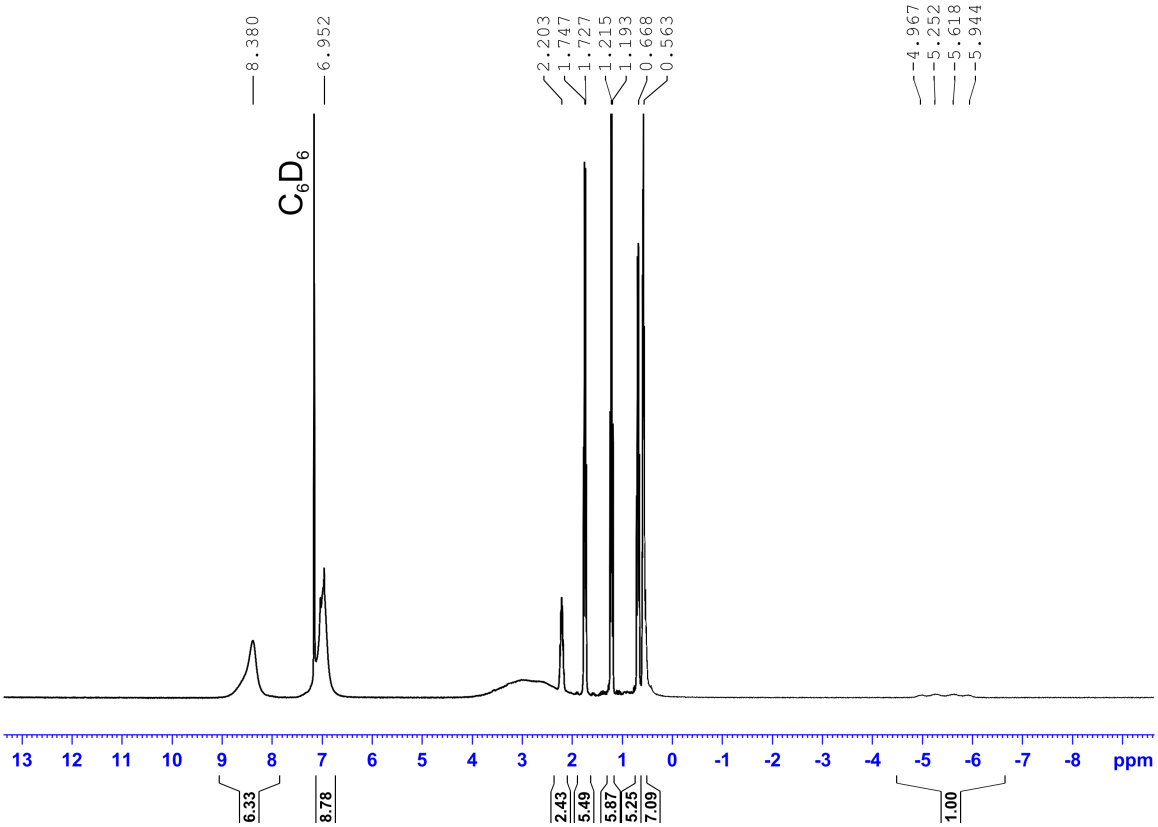

Figure S-2. The ^{1}H NMR spectrum of (POBOP)Ru(Cl)(PPh$_3$) (**2**) in C_6D_6.

^{1}H (C_6D_6): δ 8.38 (br, 6H, P(C_6*H*$_6$)$_3$), 6.95 (br, 9H, P(C_6*H*$_6$)$_3$), 4.0–1.5 (br m, 10H, B*H*), 2.20 (m, 2H, P(C*H*(CH$_3$)$_2$), 1.73 (m, 6H, P(CH(C*H*$_3$)$_2$), 1.20 (m, 6H, P(CH(C*H*$_3$)$_2$), 0.66 (m, 6H, P(CH(C*H*$_3$)$_2$), 0.56 (overlapping m, 6H, P(CH(C*H*$_3$)$_2$ and m, 2H, P(C*H*(CH$_3$)$_2$), –5.44 (q, 1H, $^1J_{BH}$ = 116 Hz B–*H*···Ru).

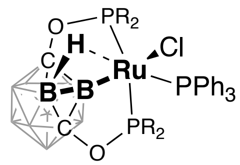

(POBOP)Ru(Cl)(PPh$_3$)

2

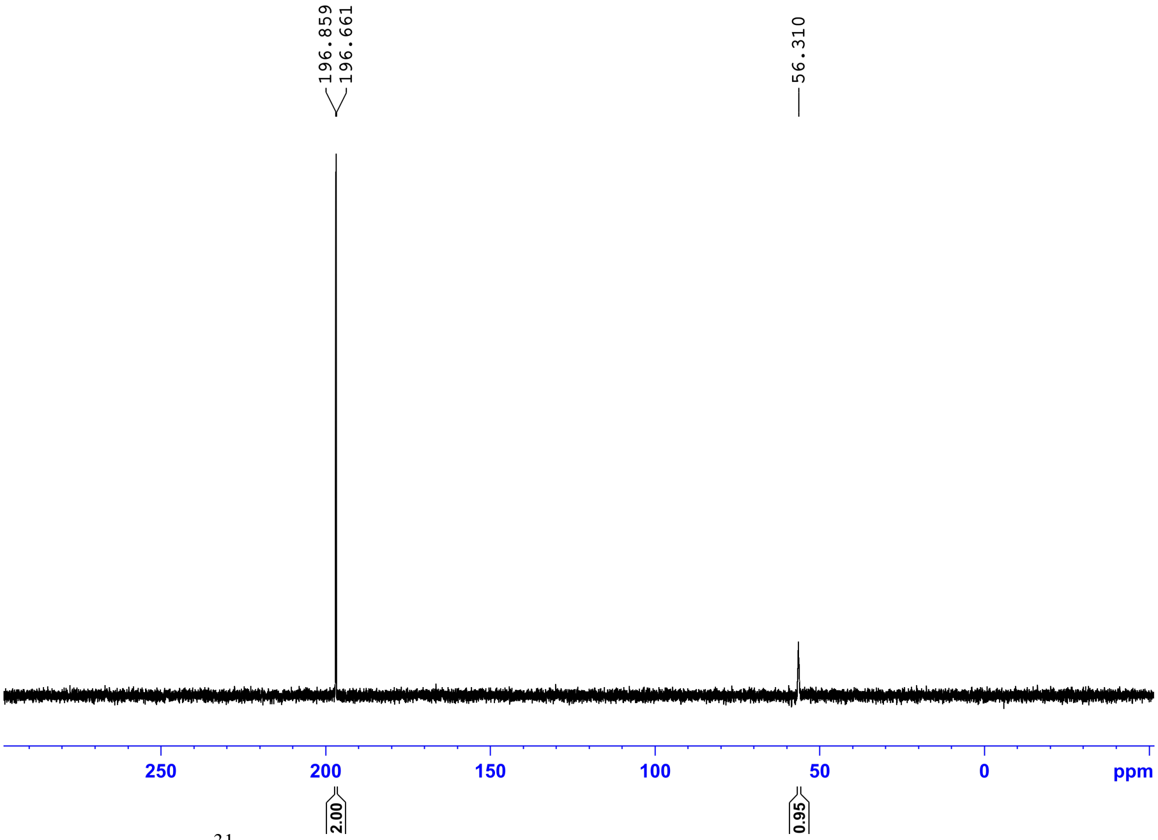

Figure S-3. The ^{31}P NMR spectrum of (POBOP)Ru(Cl)(PPh$_3$) (**2**) in C_6D_6.

$^{31}P\{^1H\}$ (C_6D_6): δ 196.8 (d, 2P, $^2J_{PP}$ = 40 Hz, *P*(CH(CH$_3$)$_2$), 56.3 (br, 1P, *P*(C_6H_6)$_3$).

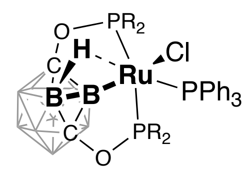

(POBOP)Ru(Cl)(PPh$_3$)

2

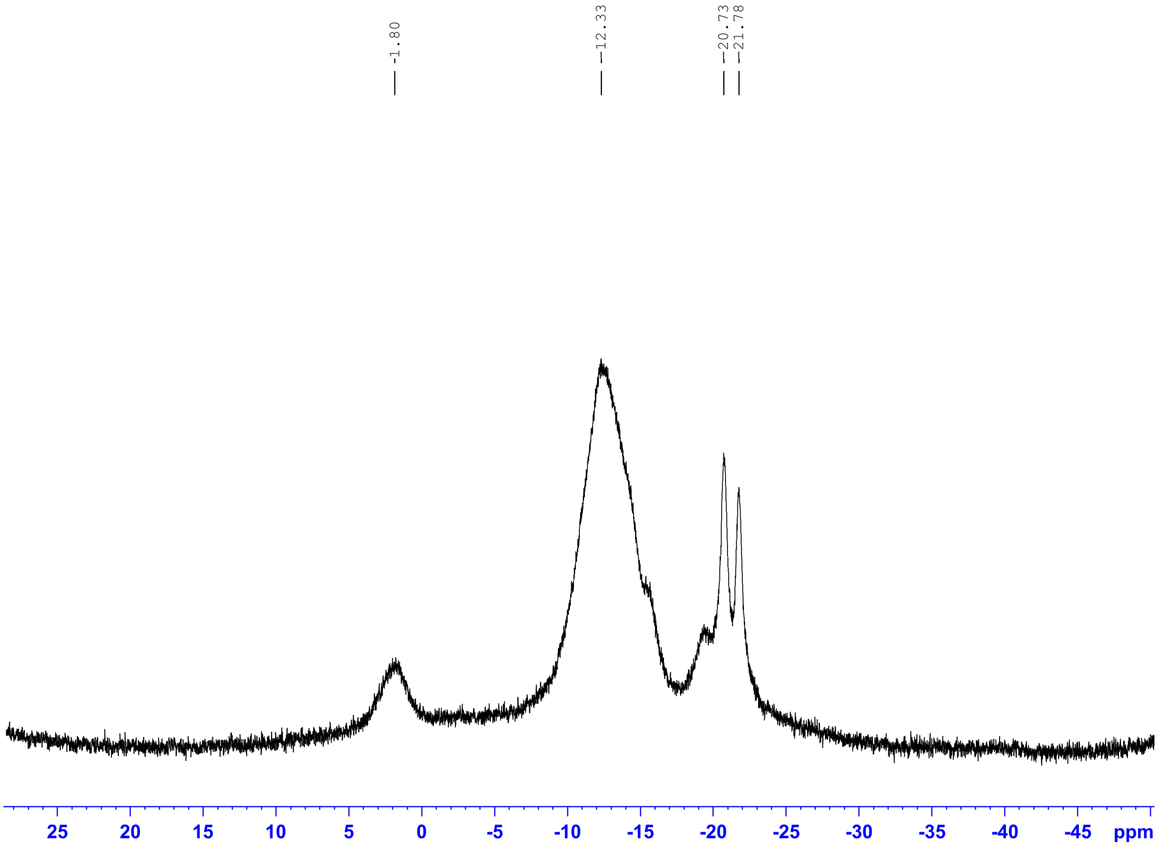

Figure S-4. The ^{11}B NMR spectrum of (POBOP)Ru(Cl)(PPh$_3$) (**2**) in C_6D_6.

^{11}B (C_6D_6): δ –1.8 (Ru–*B*), –12.3 (B–*H*), –21.3 (d, $^1J_{BH}$ = 132 Hz, B–*H*).

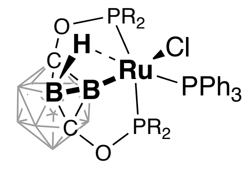

(POBOP)Ru(Cl)(PPh_3)

2

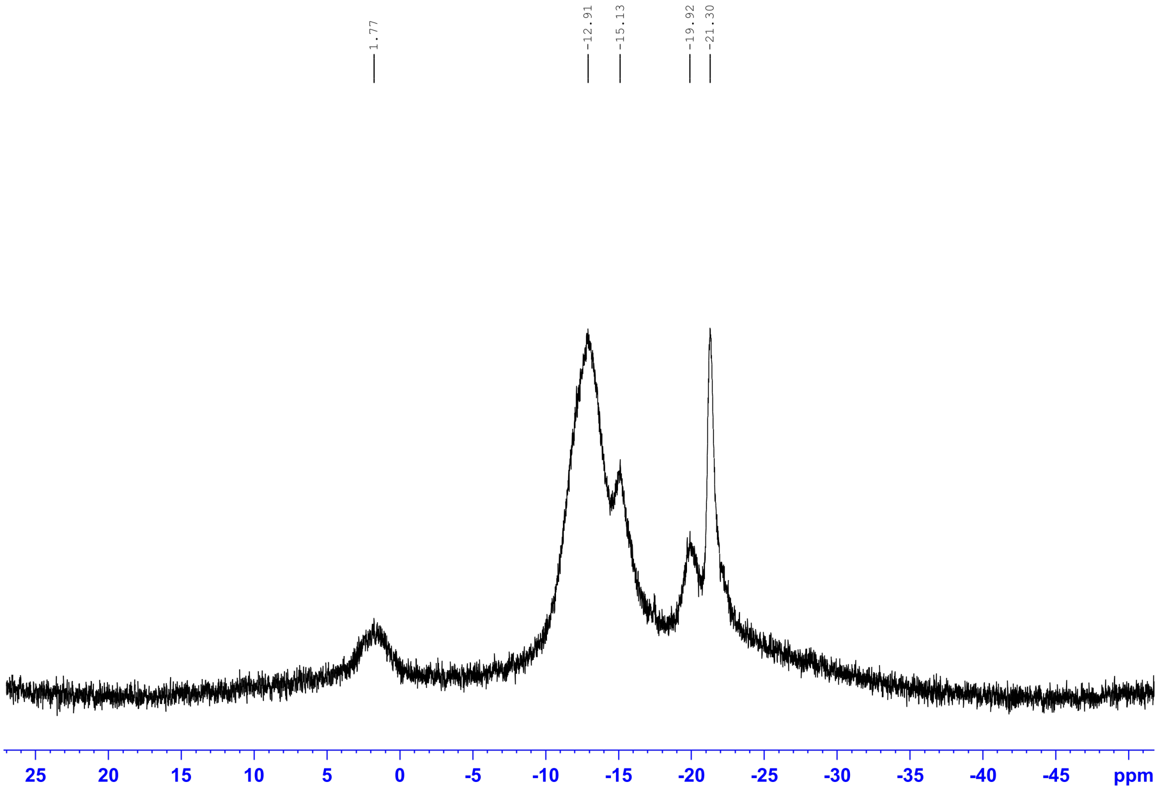

Figure S-5. The $^{11}B\{^1H\}$ NMR spectrum of (POBOP)Ru(Cl)(PPh_3) (**2**) in C_6D_6.

$^{11}B\{^1H\}$ (C_6D_6): δ –1.8 (Ru–*B*), –12.9, –15.1, –19.9, –21.3.

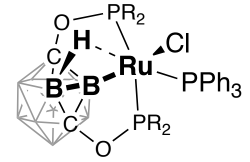

(POBOP)Ru(Cl)(PPh_3)

2

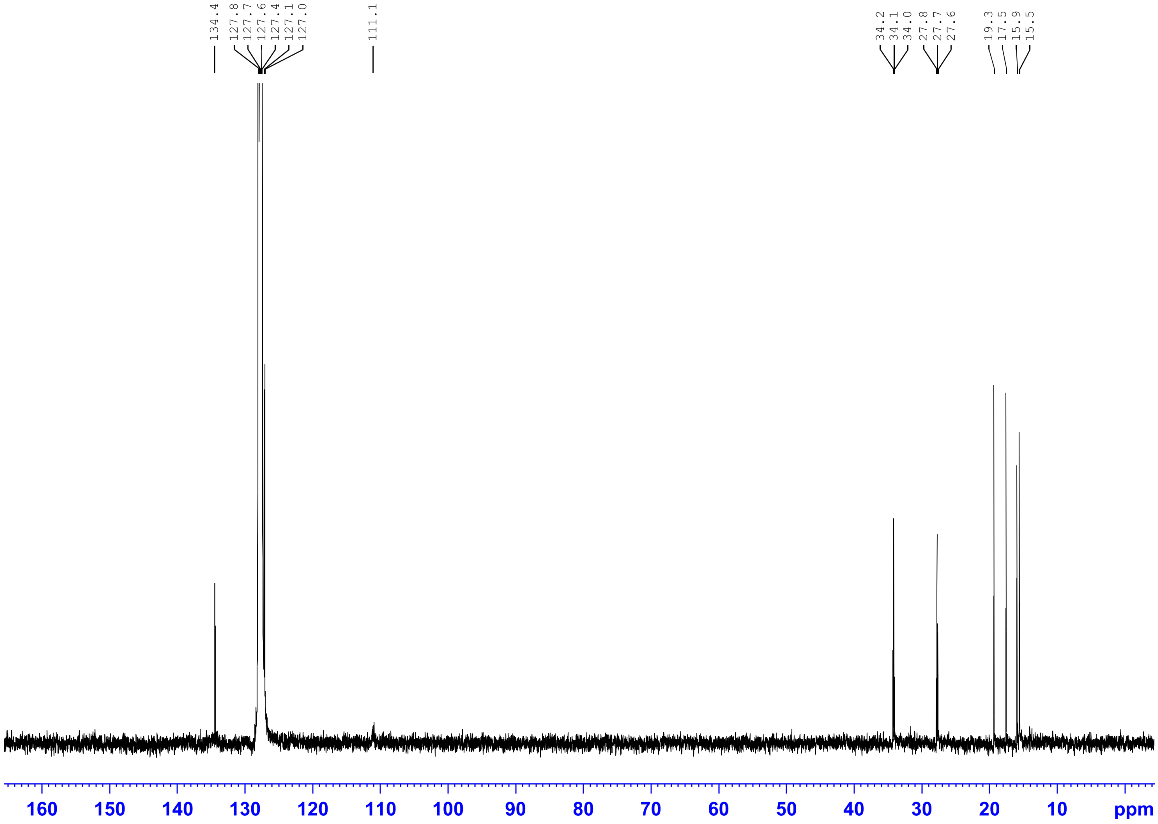

Figure S-6. The ^{1}H NMR spectrum of (POBOP)Ru(Cl)(PPh_3) (**2**) in C_6D_6.

^{13}C (C_6D_6): δ 134.4 ($P(C_6H_5)_3$, 127.0 134.4 ($P(C_6H_5)_3$, 111.1 ($C_2B_{10}H_8$), 34.1 ($P(CH(CH_3)_2$), 27.7 ($P(CH(CH_3)_2$), 19.3 ($P(CH(CH_3)_2$), 17.5 ($P(CH(CH_3)_2$), 15.9 ($P(CH(CH_3)_2$), 15.5 ($P(CH(CH_3)_2$).

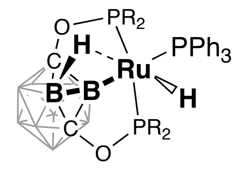

(POBOP)Ru(H)(PPh$_3$)
3

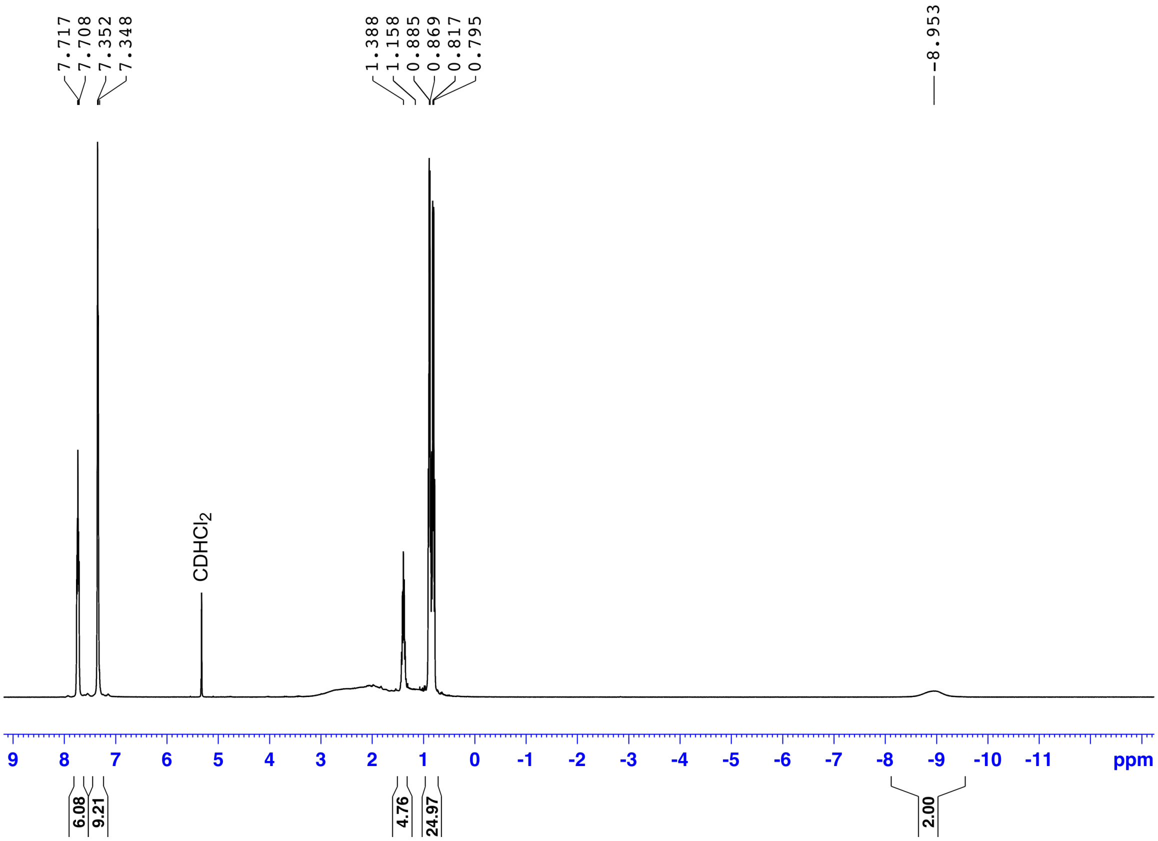

Figure S-7. The ^{1}H NMR spectrum of (POBOP)Ru(H)(PPh$_3$) (**3**) in CD$_2$Cl$_2$.

^{1}H NMR (CD$_2$Cl$_2$): δ 7.72 (m, 6H, P(C$_6$*H*$_5$)$_3$), 7.35 (m, 9H, P(C$_6$*H*$_5$)$_3$), 3.5 to 0.5 (br, 9H, C$_2$B$_{10}$*H*$_9$), 1.38 (m, 4H, P(C*H*(CH$_3$)$_2$), 0.87 (m, 12H, P(C*H*(CH$_3$)$_2$), 0.80 (m, 12H, P(CH(C*H*$_3$)$_2$)), –8.95 (br, 2H, Ru–*H*/B–*H*···Ru).

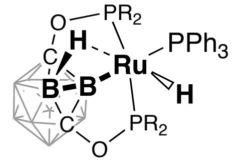

(POBOP)Ru(H)(PPh_3)

3

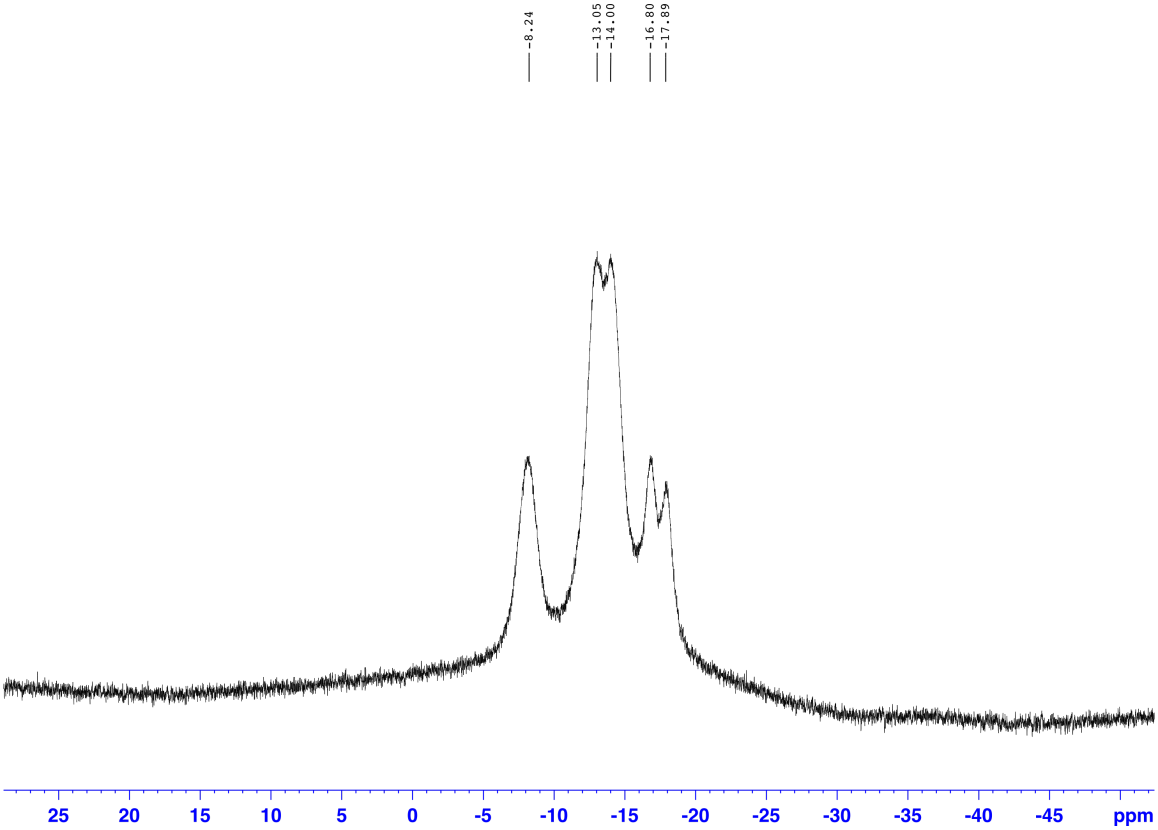

Figure S-8. The ^{11}B NMR spectrum of (POBOP)Ru(H)(PPh_3) (**3**) in CD_2Cl_2.

^{11}B{^{1}H} (CD_2Cl_2): δ –8.2 (*B*–Ru/*B*–H···Ru), –13.5 (*B*H), –17.3 (*B*H).

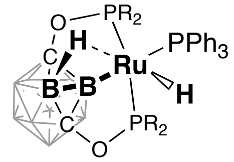

(POBOP)Ru(H)(PPh$_3$)

3

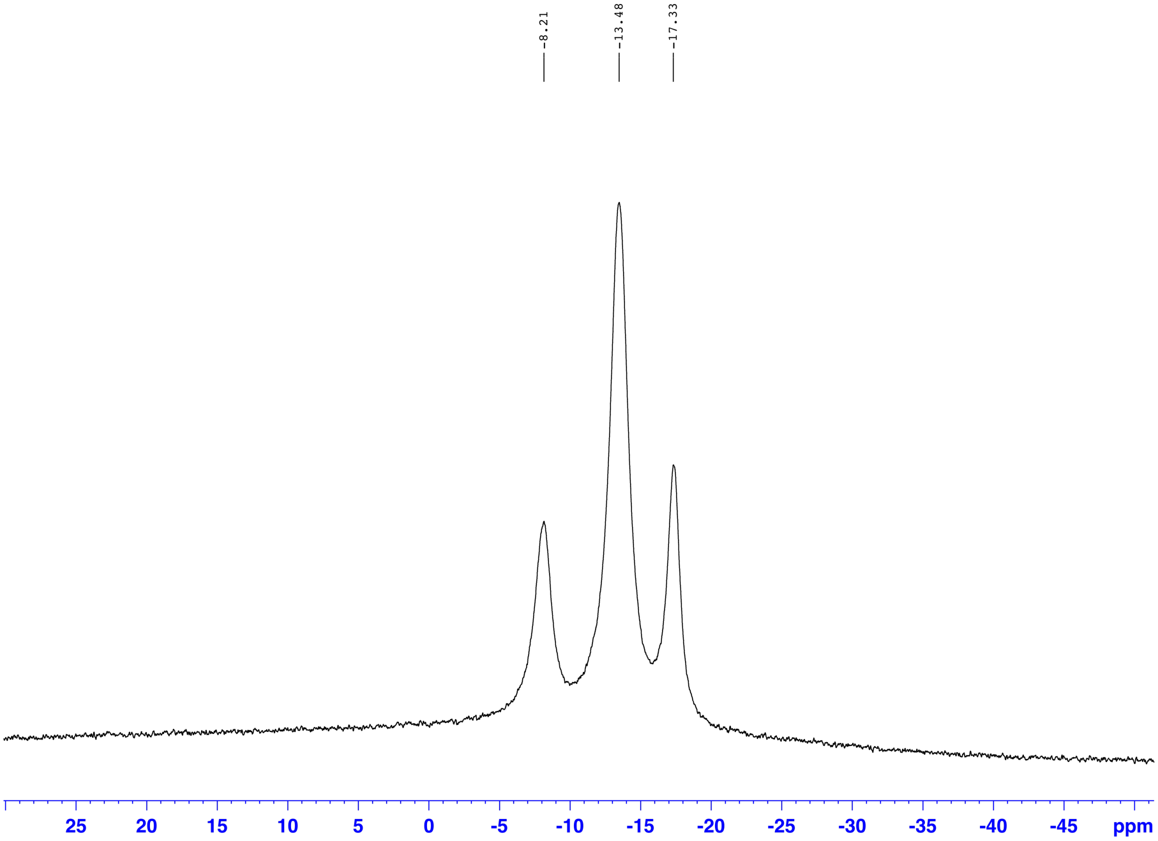

Figure S-9. The $^{11}B\{^1H\}$ NMR spectrum of (POBOP)Ru(H)(PPh$_3$) (**3**) in CD_2Cl_2.

$^{11}B\{^1H\}$ (CD_2Cl_2): δ –8.2 (*B*–Ru/*B*–H···Ru), –13.5 (*B*H), –17.3 (*B*H).

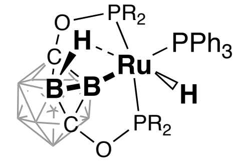

(POBOP)Ru(H)(PPh$_3$)

3

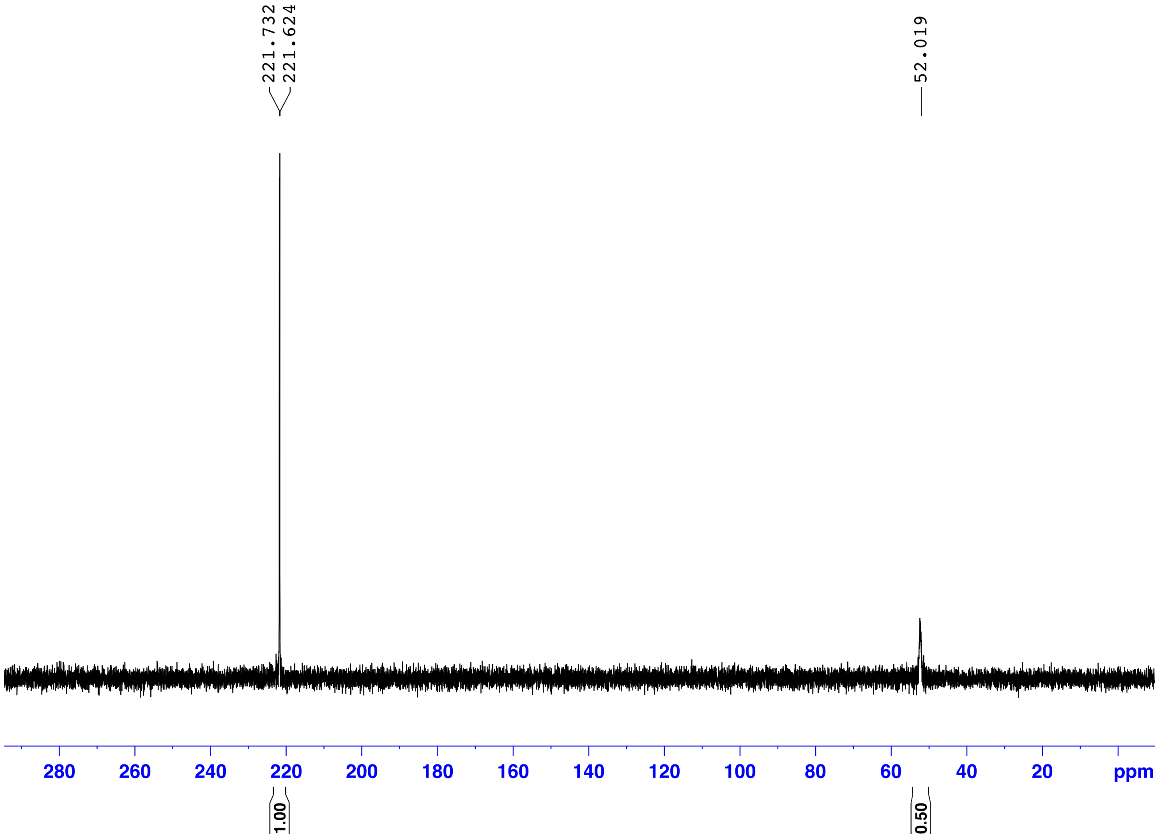

Figure S-10. The ^{31}P NMR spectrum of (POBOP)Ru(H)(PPh$_3$) (**3**) in CD$_2$Cl$_2$.

^{31}P{^{1}H} (CD$_2$Cl$_2$): δ 221.7 (d, $^2J_{PP}$ = 17 Hz, 2P, P(CH(CH_3)$_2$), 52.0 (br, 1P, P(C$_6$H$_5$)$_3$).

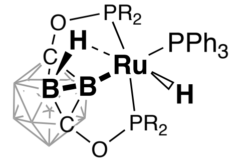

(POBOP)Ru(H)(PPh$_3$)

3

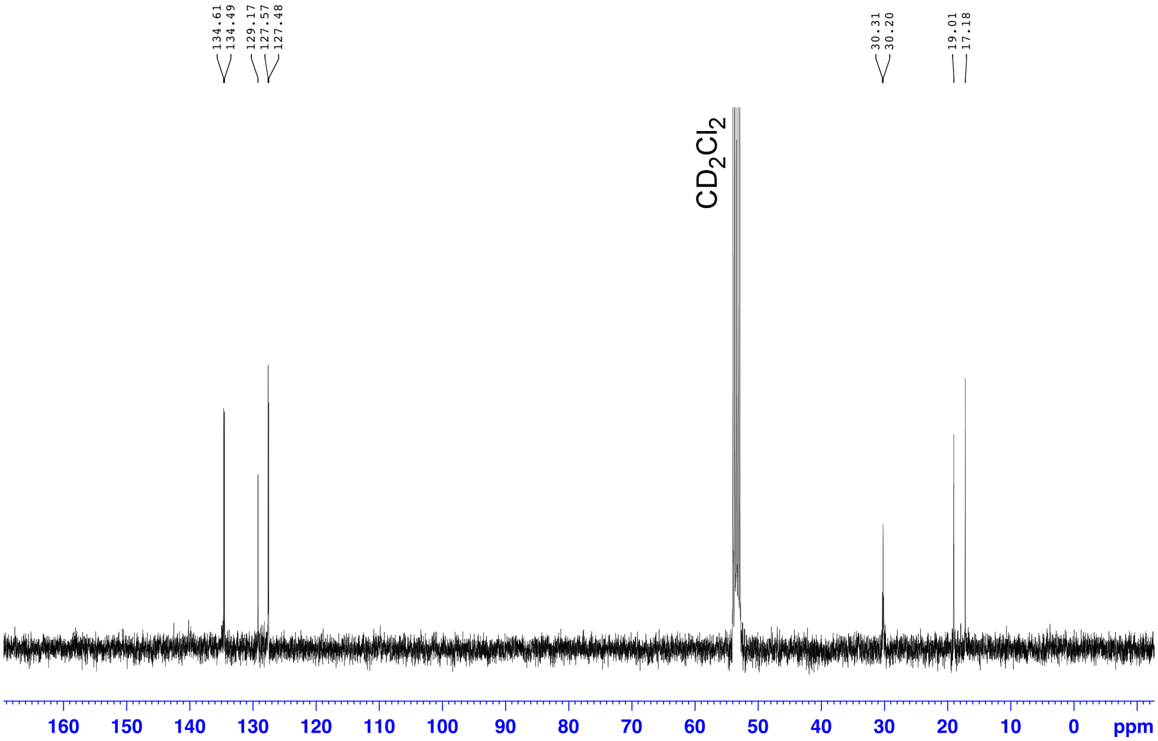

Figure S-11. The ^{13}C NMR spectrum of (POBOP)Ru(H)(PPh$_3$) (**3**) in CD$_2$Cl$_2$.

^{13}C (CD$_2$Cl$_2$): δ 134.5 (d, $^3J_{PC}$ = 12 Hz, P(C_6H$_5$)$_3$), 129.2 (P(C_6H$_5$)$_3$), 127.5 (d, $^2J_{PC}$ = 8 Hz, P(C_6H$_5$)$_3$), 30.2 (P(CH(CH$_3$)$_2$), 19.0 (P(CH(CH$_3$)$_2$), 17.2 (P(CH(CH$_3$)$_2$).

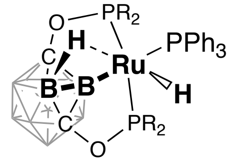

(POBOP)Ru(H)(PPh_3)

3

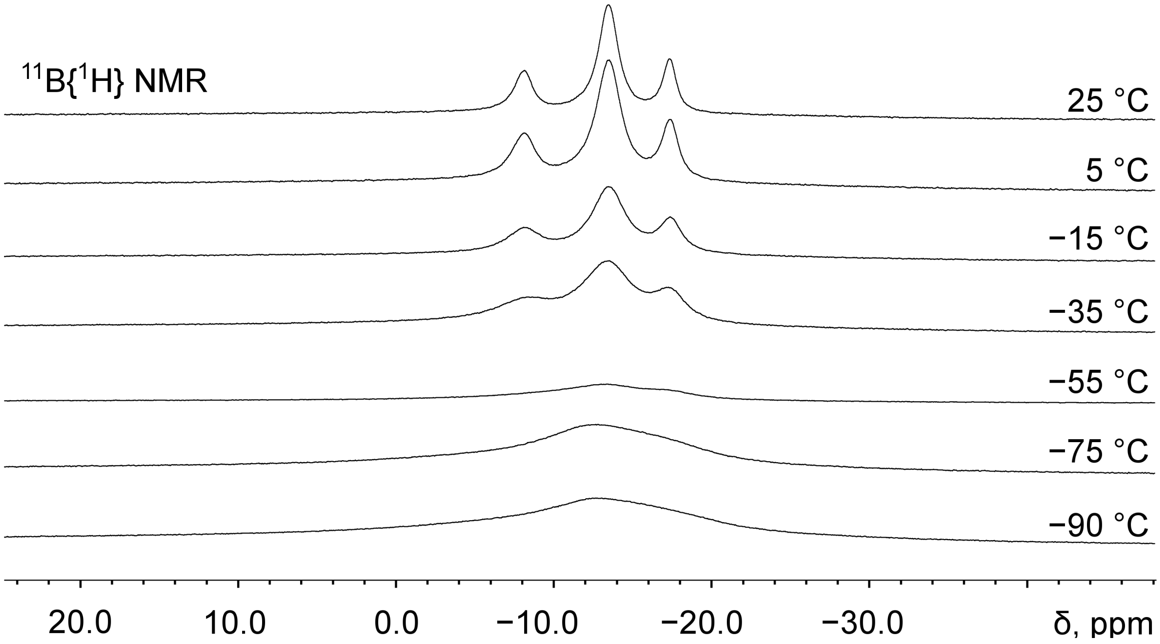

Figure S-12. The $^{11}B\{^1H\}$ NMR spectra of (POBOP)Ru(H)(PPh_3) (**3**) in CD_2Cl_2 in the temperature range from +25 ºC to –90 ºC.

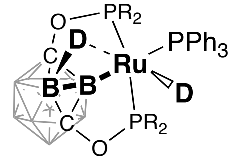

(POBOP)Ru(D)(PPh$_3$)

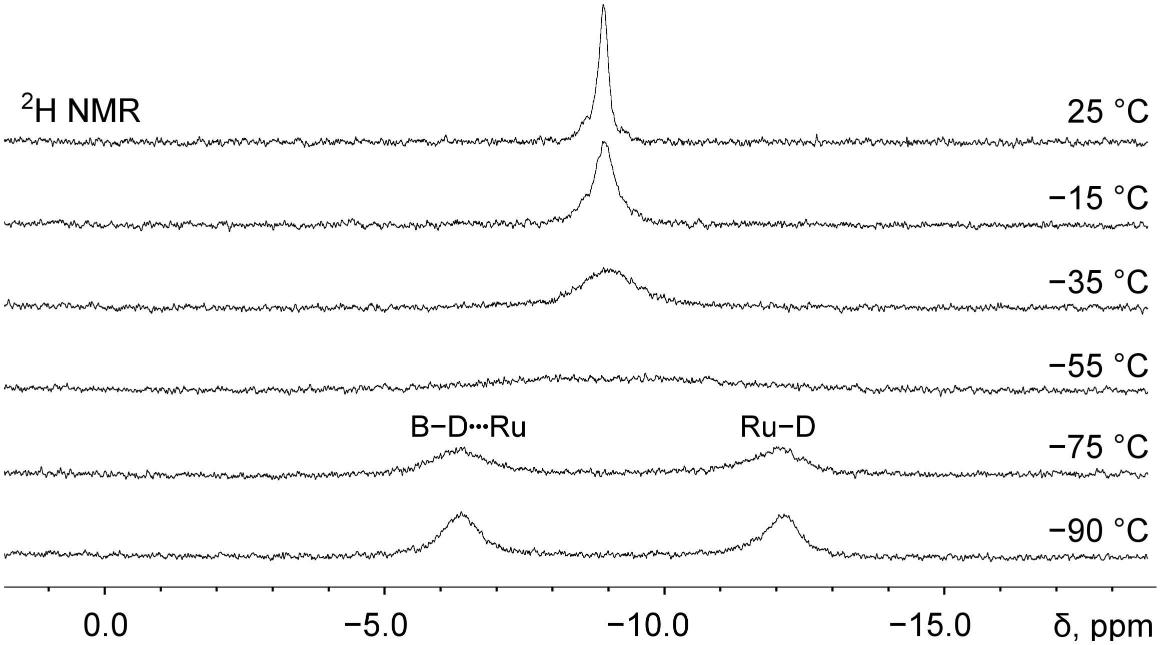

Figure S-13. The ^{2}H NMR spectra of (POBOP)Ru(D)(PPh$_3$) (**3-*d*$_2$**) in CD_2Cl_2 in the temperature range from +25 ºC to –90 ºC.

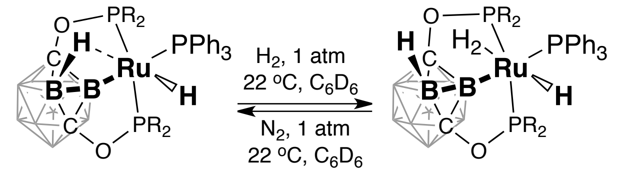

(POBOP)Ru(H)(PPh$_3$) **3** ⇌ (POBOP)Ru(H)(H$_2$)(PPh$_3$) **5**

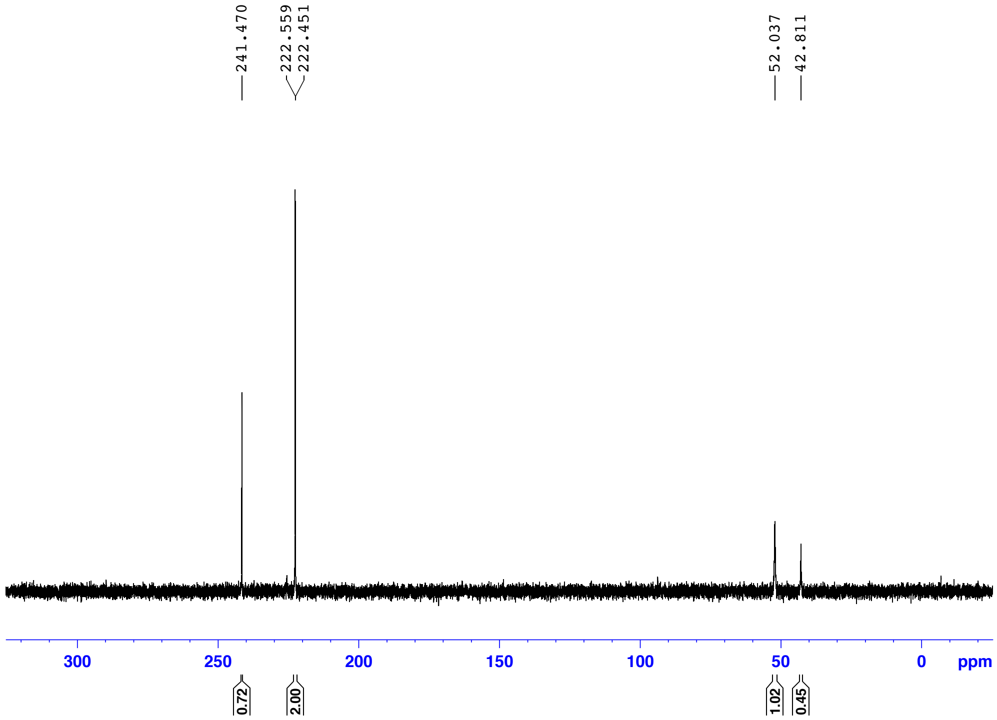

Figure S-14. The ^{31}P NMR spectrum of (POBOP)Ru(H)(PPh$_3$) (**3**) under 1 atm of H_2 in CD_2Cl_2 at –30 ºC. The signals at 222.5 ppm and 52.0 ppm correspond to the starting complex, the signals at 241.5 and 42.8 ppm correspond to a product, tentatively assigned as the (POBOP)(Ru)(H)(H$_2$)(PPh$_3$) complex (**5**).

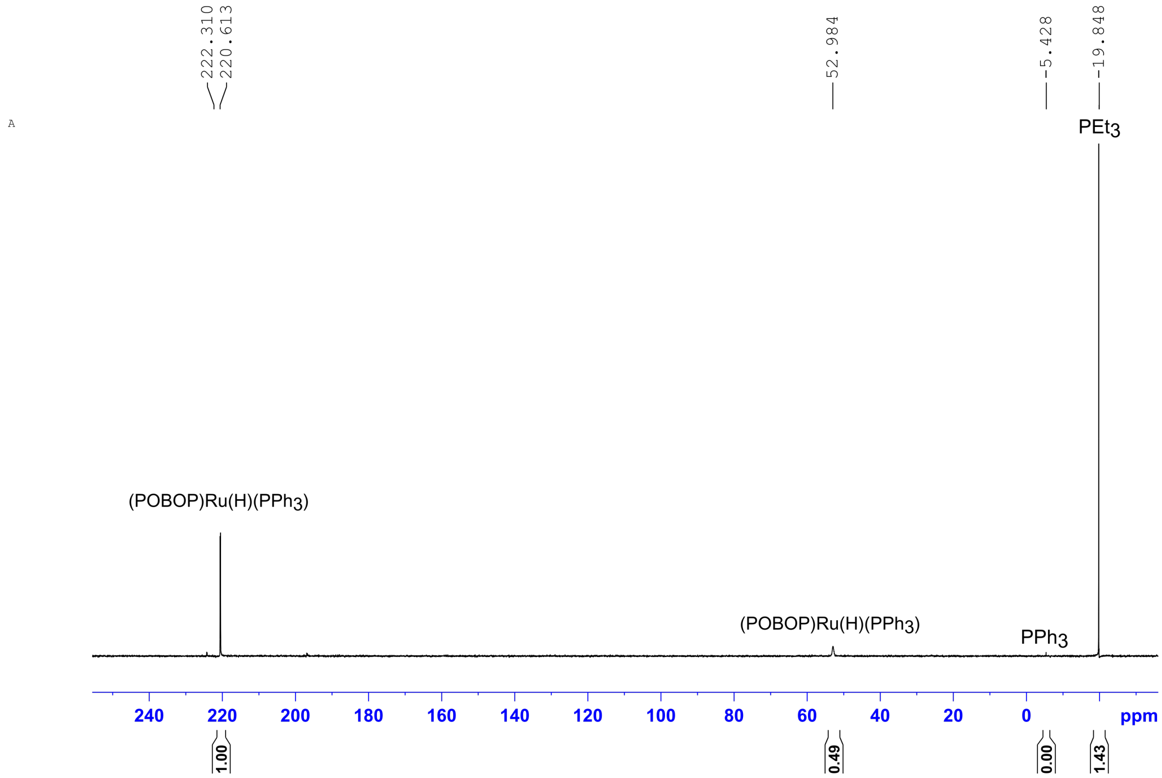

Figure S-15. The ^{31}P NMR spectrum of the mixture of (POBOP)Ru(H)(PPh_3) (**3**) and PEt_3 at room temperature in C_6D_6. The spectrum was taken 16 h after the addition of the phosphine. No significant displacement of the coordinated PPh_3 ligand (the signal at 53 ppm) by PEt_3 was observed.

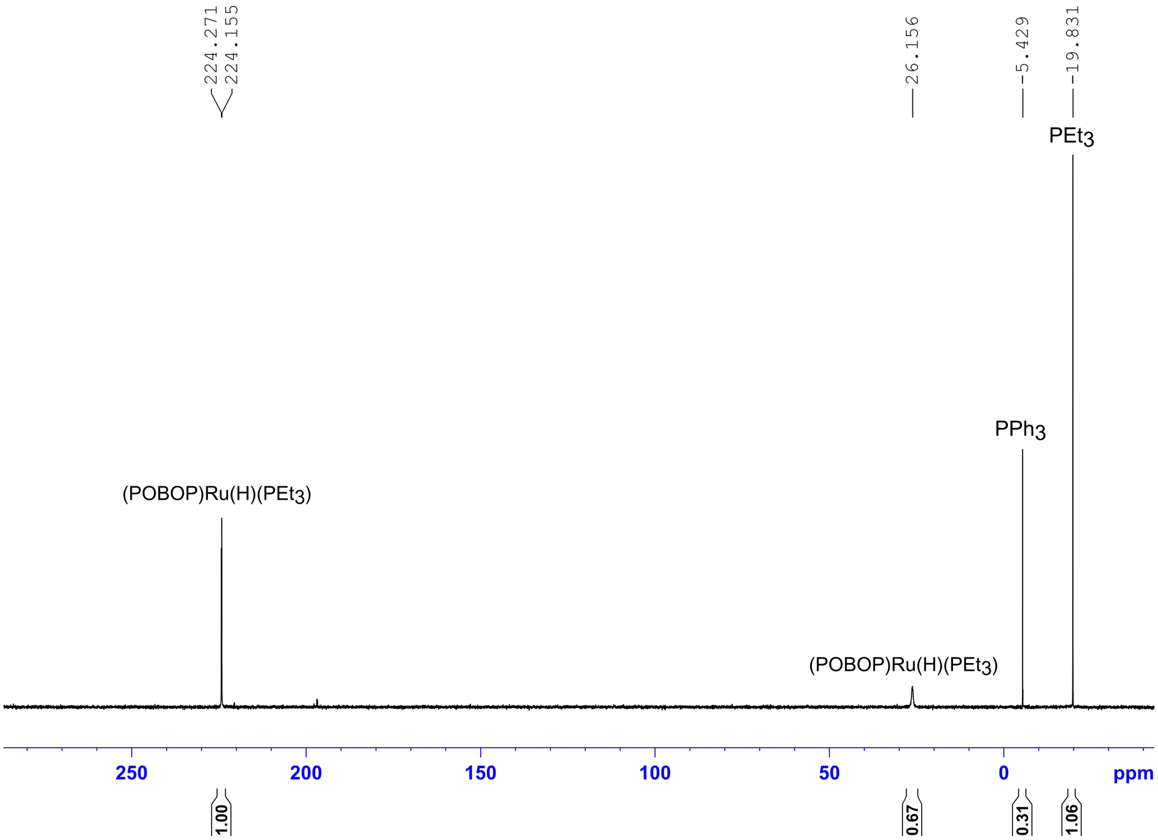

Figure S-16a. The ^{31}P NMR spectrum of the mixture of (POBOP)Ru(H)(PPh_3) (**3**) and PEt_3 in C_6D_6. The spectrum was taken after heating the mixture at 90º C for 1 h. The coordinated PPh_3 ligand was completely displaced by PEt_3.

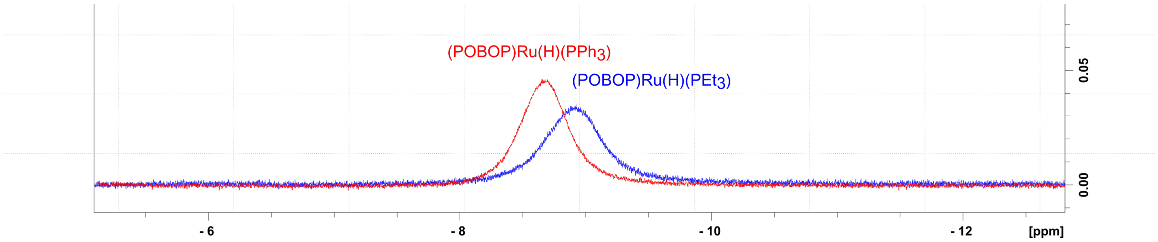

Figure S-16b. Fragments of the ^{1}H NMR spectra of the parent (POBOP)Ru(H)(PPh_3) (**3**) and (POBOP)Ru(H)(PEt_3) in C_6D_6. Note that both complexes exhibit similar dynamic behavior caused by the Ru–H/B–H···Ru exchange.

Theoretical Calculations.

Optimization of molecular structures and 2D potential energy surface scan were first performed at the PBE/TZ2P level with the Priroda code.[1, 2] For the topological analysis of the electron density with the QTAIM approach, the structure were re-optimized at the PBE0/def2-TZVP approach with ZORA correction as implemented in Orca 3.0.3 suite.[3, 4] QTAIM analysis was then performed with the use of AIMAll code,[5] Laplacian maps were visualized with Multiwfn 3.3.9 software.[6]

References.

1. D. N. Laikov and Y. A. Ustynuk, *Russ. Chem. Bull.*, 2005, **54**, 820-826.
2. D. N. Laikov, *Chem. Phys. Lett.*, 1997, **281**, 151-156.
3. F. Neese, *WIREs Comput. Mol. Sci.*, 2012, **2**, 73-78.
4. D. A. Pantazis, X.-Y. Chen, C. R. Landis and F. Neese, *J. Chem. Theory Comput.*, 2008, **4**, 908-919.
5. T. A. Keith, in *AIMAll (Version 14.04.17), http://aim.tkgristmill.com*, 2014.
6. T. Lu and F. Chen, *J. Comput. Chem.*, 2012, **33**, 580-592.

X-Ray Structure Determination, (POBOP)Ru(Cl)(PPh_3) (2)

X-ray intensity data from an orange wedge-shaped plate were collected at 100(2) K using a Bruker D8 QUEST diffractometer equipped with a PHOTON 100 CMOS area detector and an Incoatec microfocus source (Mo Kα radiation, $\lambda = 0.71073$ Å).[1] The raw area detector data frames were reduced and corrected for absorption effects using the SAINT+ and SADABS programs.[1] Final unit cell parameters were determined by least-squares refinement of 9975 reflections taken from the data set. The structure was solved by direct methods with SHELXT.[2] Subsequent difference Fourier calculations and full-matrix least-squares refinement against F^2 were performed with SHELXL-2014[2] using OLEX2.[3]

The compound crystallizes in the monoclinic system. The pattern of systematic absences in the intensity data was consistent with the space group $P2_1/n$, which was confirmed by structure solution. The asymmetric unit consists of one molecule. All non-hydrogen atoms were refined with anisotropic displacement parameters. Hydrogen atoms bonded to carbon were located in Fourier difference maps before being placed in geometrically idealized positions included as riding atoms with d(C-H) = 1.00 Å and U_{iso}(H) = 1.2U_{eq}(C) for methine hydrogen atoms, d(C-H) = 0.95 Å and U_{iso}(H) = 1.2U_{eq}(C) for arene hydrogens and d(C-H) = 0.98 Å and U_{iso}(H) = 1.5U_{eq}(C) for methyl hydrogens. The methyl hydrogens were allowed to rotate as a rigid group to the orientation of maximum observed electron density. Hydrogen atoms bonded to boron were located in difference maps and refined freely. Special attention was given to the difference electron density in the regions of boron atoms B1 and B2. No density above background was observed near B1, while a peak of magnitude 1.0 $e^-/Å^3$, was observed at *ca*. 1.12 Å from B2. This refined well as B-Ru bridging hydrogen H2, resulting in reasonable B-H, Ru-H distances and H2 displacement parameter. The largest residual electron density peak in the final difference map is 0.57 $e^-/Å^3$, located 0.66 Å from Cl1.

---

1. APEX2 Version 2014.9-0, SAINT+ Version 8.34A and SADABS Version 2014/4. Bruker Analytical X-ray Systems, Inc., Madison, Wisconsin, USA, 2014.

2. (a) **SHELXT**: Sheldrick, G. M. *Acta Cryst.* **2015**, *A71*, 3-8. (b) **SHELXL:** Sheldrick, G. M. *Acta Cryst.* **2008**, *A64*, 112-122.

3. Dolomanov, O. V.; Bourhis, L. J.; Gildea, R. J.; Howard J. A. K.; Puschmann, H. *J. Appl. Cryst.* **2009**, *42*, 339-341.

Table S-1. Crystal data and structure refinement for (POBOP)Ru(Cl)(PPh_3) (**2**)

Identification code	BE2178
Empirical formula	$C_{32}H_{52}B_{10}ClO_2P_3Ru$
Formula weight	806.26
Temperature/K	100(2)
Crystal system	monoclinic
Space group	$P2_1/n$
a/Å	12.4465(4)
b/Å	23.0308(8)
c/Å	13.2665(4)
α/°	90
β/°	96.2390(10)
γ/°	90
Volume/Å^3	3780.4(2)
Z	4
ρ_{calc}g/cm^3	1.417
μ/mm^{-1}	0.643
F(000)	1664.0
Crystal size/mm^3	0.22 × 0.16 × 0.04
Radiation	MoKα (λ = 0.71073)
2Θ range for data collection/°	4.614 to 60.158
Index ranges	$-17 \leq h \leq 17$, $-32 \leq k \leq 32$, $-18 \leq l \leq 18$
Reflections collected	214626
Independent reflections	11098 [R_{int} = 0.0557, R_{sigma} = 0.0242]
Data/restraints/parameters	11098/0/487
Goodness-of-fit on F^2	1.033
Final R indexes [I>=2σ (I)]	R_1 = 0.0248, wR_2 = 0.0568
Final R indexes [all data]	R_1 = 0.0373, wR_2 = 0.0603
Largest diff. peak/hole / e Å^{-3}	0.57/-0.72

X-Ray Structure Determination, (POBOP)Ru(H)(PPh_3) (3)

X-ray intensity data from an irregular colorless plate were collected at 100(2) K using a Bruker D8 QUEST diffractometer equipped with a PHOTON 100 CMOS area detector and an Incoatec microfocus source (Mo Kα radiation, $\lambda = 0.71073$ Å).[1] The raw area detector data frames were reduced and corrected for absorption effects using the SAINT+ and SADABS programs.[1] Final unit cell parameters were determined by least-squares refinement of 9978 reflections taken from the data set. The structure was solved by direct methods with SHELXT.[2] Subsequent difference Fourier calculations and full-matrix least-squares refinement against F^2 were performed with SHELXL-2014[2] using OLEX2.[3]

The compound crystallizes in the triclinic system. The space group *P*-1 was confirmed by structure solution. The asymmetric unit consists of two chemically similar but crystallographically independent molecules. The two unique molecules were numbered identically except for label suffixes A or B. All non-hydrogen atoms were refined with anisotropic displacement parameters. Hydrogen atoms bonded to carbon were located in Fourier difference maps before being placed in geometrically idealized positions included as riding atoms with d(C-H) = 1.00 Å and $U_{iso}(H) = 1.2U_{eq}(C)$ for methine hydrogen atoms, d(C-H) = 0.95 Å and $U_{iso}(H) = 1.2U_{eq}(C)$ for arene hydrogens and d(C-H) = 0.98 Å and $U_{iso}(H) = 1.5U_{eq}(C)$ for methyl hydrogens. The methyl hydrogens were allowed to rotate as a rigid group to the orientation of maximum observed electron density. Hydrogen atoms bonded to boron were located in difference maps; most were refined freely. The displacement parameters for three (H5B, H6B, H9B) were treated as riding to prevent abnormally small values. Special attention was given to the difference electron density in the regions of boron atoms B1 and B2 of each independent molecule. No density above background was observed near the B1 atoms, while significant peaks were observed at *ca.* 1.2 Å from B2. These both refined well as B-Ru bridging hydrogen atoms H2(A/B), resulting in reasonable B-H, Ru-H distances and H2 displacement parameters. The two unique hydride atoms H1(A/B) were also located and refined freely. The largest residual electron density peak in the final difference map is 0.63 $e^-/Å^3$, located 0.99 Å from H1A.

1. APEX2 Version 2014.9-0, SAINT+ Version 8.34A and SADABS Version 2014/4. Bruker Analytical X-ray Systems, Inc., Madison, Wisconsin, USA, 2014.

2. (a) **SHELXT**: Sheldrick, G. M. *Acta Cryst.* **2015**, *A71*, 3-8. (b) **SHELXL:** Sheldrick, G. M. *Acta Cryst.* **2008**, *A64*, 112-122.

3. Dolomanov, O. V.; Bourhis, L. J.; Gildea, R. J.; Howard J. A. K.; Puschmann, H. *J. Appl. Cryst.* **2009**, *42*, 339-341.

Table S-2. Crystal data and structure refinement for (POBOP)Ru(H)(PPh_3) (**3**)

Identification code	BE2199
Empirical formula	$C_{32}H_{53}B_{10}O_2P_3Ru$
Formula weight	771.82
Temperature/K	100(2)
Crystal system	triclinic
Space group	$P\bar{1}$
a/Å	12.5744(5)
b/Å	15.5222(7)
c/Å	19.5052(8)
α/°	88.2590(10)
β/°	81.9880(10)
γ/°	89.388(2)
Volume/Å^3	3768.1(3)
Z	4
ρ_{calc}g/cm^3	1.361
μ/mm^{-1}	0.573
F(000)	1600.0
Crystal size/mm^3	0.18 × 0.08 × 0.02
Radiation	MoKα (λ = 0.71073)
2Θ range for data collection/°	4.438 to 52.776
Index ranges	$-15 \le h \le 15$, $-19 \le k \le 19$, $-24 \le l \le 24$
Reflections collected	82388
Independent reflections	15369 [R_{int} = 0.0898, R_{sigma} = 0.0734]
Data/restraints/parameters	15369/0/959
Goodness-of-fit on F^2	1.045
Final R indexes [I>=2σ (I)]	R_1 = 0.0372, wR_2 = 0.0707
Final R indexes [all data]	R_1 = 0.0663, wR_2 = 0.0782
Largest diff. peak/hole / e Å^{-3}	0.63/-0.62